

# ORDINAL PROBIT FUNCTIONAL REGRESSION MODELS WITH APPLICATION TO COMPUTER-USE BEHAVIOR IN RHESUS MONKEYS\*

BY MARK J. MEYER<sup>†</sup>, JEFFREY S. MORRIS<sup>‡</sup>, REGINA PAXTON GAZES<sup>§</sup>,  
ROBERT R. HAMPTON<sup>¶,||</sup> AND BRENT A. COULL<sup>\*\*</sup>

*Georgetown University<sup>†</sup>, The University of Texas MD Anderson Cancer  
Center<sup>‡</sup>, Bucknell University<sup>§</sup>, Emory University<sup>¶</sup>, Yerkes National  
Primate Research Center<sup>||</sup>, and Harvard T.H. Chan School of Public  
Health<sup>\*\*</sup>*

Research in functional regression has made great strides in expanding to non-Gaussian functional outcomes, however the exploration of ordinal functional outcomes remains limited. Motivated by a study of computer-use behavior in rhesus macaques (*Macaca mulatta*), we introduce the Ordinal Probit Functional Regression Model or OPFRM to perform ordinal function-on-scalar regression. The OPFRM is flexibly formulated to allow for the choice of different basis functions including penalized B-splines, wavelets, and O’Sullivan splines. We demonstrate the operating characteristics of the model in simulation using a variety of underlying covariance patterns showing the model performs reasonably well in estimation under multiple basis functions. We also present and compare two approaches for conducting posterior inference showing that joint credible intervals tend to out perform point-wise credible. Finally, in application, we determine demographic factors associated with the monkeys’ computer use over the course of a year and provide a brief analysis of the findings.

**1. Introduction.** Gazes et al. (2013) presents a study of computer-use patterns in a socially-housed group of rhesus macaques (*Macaca mulatta*) at the Yerkes National Primate Research Center in Atlanta, GA who were given access to automated touch-screen computer systems between March 2009 and April 2014. Usage data was collected for all non-infant monkeys in the colony for this period. Each animal had an RFID implant that was read by the computer on each trial, and used to track individual computer use. The raw data that was collected is the amount of time each monkey spends during a session using the touch-screens each day. While the raw data can be

---

\*This work was supported by grants from the National Institutes of Health (ES-007142, ES-000002, CA-134294, CA-178744, R01MH081862), the National Science Foundation (#IOS-1146316), and ORIP/OD (P51OD011132).

*Keywords and phrases:* Functional Data Analysis, Generalized Outcomes, Wavelets, Penalized Splines, O’Sullivan Splines, Probit Regression

considered continuous, the broader trends of usage on an ordinal scale, such as no usage, low usage, moderate usage, and high usage have more practical value for psychologists making choices about which individuals will be productive research subjects. Additionally, these classifications are particularly important for assessing what types of comparative research questions can be asked in the population. For example, if the researcher is interested in comparing cognitive performance based on dominance rank, but low ranking animals show low or no usage, the researcher will not be able to collect sufficient data to address this question in this population.

Using this data, we wish to identify factors that are associated with how much a monkey uses the system on a given day—using the aforementioned scale—and how that usage changes over the course of the year, from September through August. The outcome of interest is daily usage of the touchscreens and is both functional and ordinal. Our goal is to relate this outcome to a set of demographic variables of interest that includes rank within the group, sex, and age, all of which are scalars. This will allow psychologists to determine which demographic groups produce sufficient subject numbers for cognitive tests. This information is valuable when studying cognition using automated cognitive testing systems for animals housed in large social groups, a type of testing that is increasing in popularity due to advances in relevant technology. A reasonable choice for modeling how demographic-specific usage varies over the course of a year is then a function-on-scalar regression. We now present a review of the relevant literature.

Faraway (1997) and Ramsay and Silverman (1997) represent the early work on function-on-scalar regression, however the literature since has grown. For example, Guo (2002), Shi et al. (2007), and Reiss, Huang, and Mennes (2010) consider kernel smoothing and spline-based approaches to model a functional outcome while Krafty et al. (2008) and Scheipl, Staicu, and Greven (2015) explore the use of functional principal components. Morris (2015) provides an extensive review of function-on-scalar regression literature. In the Bayesian context, Morris and Carroll (2006) introduces Wavelet-based Functional Mixed Models (WFMM) for function-on-scalar regression while Goldsmith and Kitago (2016) use splines and functional principal components (fPC) in both fully Bayesian and variational Bayesian models. Both approaches provide flexible frameworks for modeling functional outcomes in a number of settings and several authors have extended both methodologies. Zhu, Brown, and Morris (2011, 2012) discuss robust adaptive regression and robust classification in WFMMs respectively while Meyer et al. (2015) introduces the function-on-function extension. Lee et al. (2018) extend WFMM to semi-parametric models with smooth nonparametric covariate effects in

function-on-scalar regression models. Extensions of Goldsmith and Kitago (2016) include Chen, Goldsmith, and Ogden (2016) and Goldsmith and Schwartz (2017) which examine variable selection in function-on-scalar and functional linear concurrent models, respectively. However, both frameworks can only be applied to continuous valued functional responses, and thus cannot be applied to discrete valued functions including the ordinal case that is of interest in our application.

While the literature on generalized function-on-scalar regression has expanded recently, it still remains limited in scope. Hall, Müller, and Yao (2008) extend functional principal components analysis to allow for generalized outcomes. Li, Staudenmayer, and Carroll (2014), Gertheiss et al. (2015), Scheipl, Gertheiss, and Greven (2016), and Li, Huang, and Shen (2018), develop frequentist methods for binary and count functional outcomes using GEE-type, maximum likelihood-based, quasi-likelihood based, and fPC based approaches, respectively. van der Linde (2009) proposes a Bayesian version of Hall, Müller, and Yao (2008) using a variational algorithm to obtain approximate Bayesian inference for count and binary data. van der Linde (2011) extends this approach further, proposing reduced rank models for functional canonical correlation analysis and functional discriminant analysis. More recently, Wang and Shi (2014) implement an empirical Bayesian learning approach using a Gaussian approximation and B-splines for outcomes arising from exponential families. Goldsmith, Zipunnikov, and Schrack (2015) develop a fully Bayesian model for multilevel generalized function-on-scalar regression using fPC and penalized splines for binary and count data. Much of the existing literature focuses on either the binary or Poisson case and while Wang and Shi (2014) do present a method capable of handling an ordinal functional outcome, the authors only discuss a single simulated data setting and do not explore the models operating characteristics in that context nor have they made code publicly available to implement their method. To the best of our knowledge, no previous work implements wavelet-based generalized function-on-scalar regression. Moreover, most frameworks do not allow for flexibility in choice of basis functions, preferring to work with one set of basis functions over another. The available links in the current literature are also limited with the probit link not receiving attention. Thus a gap remains in the literature for generalized function-on-scalar methods that allow for the probit link, can handle ordinal outcomes, and have multiple choices in basis function including wavelets.

To address this gap, we introduce the Ordinal Probit Functional Regression Model (OPFRM), a fully Bayesian model for regressing an ordinal functional outcome onto a set of scalar covariates. The modeling framework

utilizes a data augmentation to model an ordinal functional outcome of arbitrary level using the probit link. We also allow for a flexible choice in basis functions with both wavelet and spline based representations of the model in the spirit of [Morris and Carroll \(2006\)](#) and [Goldsmith and Kitago \(2016\)](#), respectively. As such, any discrete wavelet transformation is available for use and B-splines are one option for the spline-based model. We also allow for the use of O’Sullivan splines, described by [Wand and Ormerod \(2008\)](#), which can be more efficient than B-splines alone and have received limited use in functional regression. We formulate the OPFRM in a way that is computationally feasible even for quite large functional data sets as well as a large number of scalar covariates. We describe two MCMC algorithms for generating posterior estimates and provide MATLAB code to run all models at <https://github.com/markjmeyer/OPFRM>.

We organize the remainder of the manuscript in the following way: Section 2 presents the general OPFRM framework. Section 3 gives details on both the spline and wavelet based models. In Section 4, we discuss the results of our simulation. Section 5 is where we apply the OPFRM to the computer-use data. And in Section 6, we provide a discussion of the methodology.

**2. Ordinal Probit Functional Regression Model.** Here we detail the modeling framework for the OPFRM. Let  $Y_i(t)$  be the observed value for subject  $i$  at time  $t$ ,  $i = 1, \dots, N$  and  $t = t_1, \dots, t_T$ . Then  $Y_i(t)$  takes on one of  $L$  possible values:  $\ell = \{0, 1, \dots, L-1\}$ . In the context of the computer-use data,  $Y_i(t)$  takes on 0, 1, 2, or 3 depending on a monkey’s level of usage on day  $t$ : none, low, moderate, or high. As  $t$  only indexes measurement time,  $Y_i(t)$  need not necessarily be sampled on an equally spaced grid; however we do assume that each subject has the same number of measurements taken at approximately the same intervals. Further, without-loss of generality, let  $x_i$  represent a single scalar covariate of interest for subject  $i$ . Extension to a set of scalar covariates is straightforward.

[Albert and Chib \(1993\)](#) introduce a data augmentation strategy for modeling univariate binary, ordinal, and nominal outcomes in a Bayesian context. We use a similar approach to model the functional categorical outcome. That is, we represent  $Y_i(t)$  in terms of a continuous latent process,  $Y_i^*(t)$ .

The behavior of  $Y_i(t)$  is then specified by the relationship

$$(2.1) \quad Y_i(t) = \begin{cases} 0 & \text{if } c_0 \leq Y_i^*(t) < c_1 \\ 1 & \text{if } c_1 \leq Y_i^*(t) < c_2 \\ \vdots & \\ \ell & \text{if } c_\ell \leq Y_i^*(t) < c_{\ell+1} \\ \vdots & \\ L-1 & \text{if } c_{L-1} \leq Y_i^*(t) < c_L \end{cases}$$

for cut points  $c_0, c_1, \dots, c_\ell, \dots, c_L$ , satisfying  $c_0 < c_1 < \dots < c_\ell < \dots < c_L$ . Using the mapping in Model (2.1), the probability that  $Y_i(t)$  equals the  $\ell$ th level can be expressed as

$$(2.2) \quad P[Y_i(t) = \ell] = P[Y_i^*(t) \in (c_\ell, c_{\ell+1})], \quad \ell = 0, 1, \dots, L-1,$$

where  $c_0$  and  $c_L$  will vary depending on the support of  $Y_i^*(t)$ . We then let the form of  $Y_i^*(t)$  be the function-on-scalar regression model

$$(2.3) \quad Y_i^*(t) = x_i\beta(t) + E_i(t),$$

where  $x_i$  is a single scalar covariate although inclusion of multiple covariates is straightforward. The choice of the distribution for the errors,  $E_i(t)$ , completes the model specification.

If we assume the errors follow a Gaussian process, then by normalizing  $Y_i^*(t)$  we can re-express Model (2.2) in terms of the CDF of the standard Gaussian,  $\Phi(\cdot)$ . The probabilities at a fixed  $t$  for subject  $i$  are then

$$(2.4) \quad P[Y_i(t) = \ell] = \Phi[c_{\ell+1} - x_i\beta(t)] - \Phi[c_\ell - x_i\beta(t)]$$

for  $\ell = 0, 1, \dots, L-1$ . The Gaussian assumption results in the probit formulation of the model and  $c_0$  and  $c_L$  are defined to be  $-\infty$  and  $\infty$ , respectively.

Models (2.3) and (2.4) represent the formulation for continuous functions; however, we only observe discretized realizations of  $Y_i^*$ . Assuming all functions have the same number of measurements—not necessarily equally spaced—and no missing values, the discrete version of model (2.3), across all subjects is

$$(2.5) \quad Y^* = X\beta + E, \quad E \sim \mathcal{GP}(0, \Sigma_E),$$

where  $Y^*$  and  $E$  are  $N \times T$  matrices. If  $P$  is the number of covariates, then  $\beta$  is a  $P \times T$  matrix and  $X$  is an  $N \times P$  matrix. The first two steps of the samplers for both the wavelet and spline based models are the same. By making the error Gaussian, we assume the prior on latent variable is also Gaussian. After fixing the first cut point,  $c_1$ , typically at 0, we assume a flat prior on the remaining  $c_\ell$ ,  $\ell = 2, \dots, L-1$ .

**2.1. Identifiability.** For identifiability, the first cut point must be fixed. Further, estimation of the remaining cut points means the intercept function is not identifiable as the cut points act like global intercepts based on the level of the outcome at time  $t$ . If one wants to estimate a functional intercept, then the cut points must all be fixed. In this work, we choose to estimate the cut points, thus  $X$  does not include an intercept column. The error matrix  $\Sigma_E$  is also not identifiable due to the scale-invariance of the augmentation. In the univariate case, this is handled by assuming the errors are set to one, see [Albert and Chib \(1993\)](#). We make the analogous assumption in our model letting  $\Sigma_E = I_{T \times T}$ , the  $T \times T$  identity matrix. We do estimate  $\Sigma_E$  indirectly using a non-informative prior with estimation depending on basis choice. However, given the non-identifiability of the variance, we do not retain these samples and only allow them to supplement our estimation of the model coefficients.

**2.2. Latent Conditionals.** Based on the prior assumptions, the full conditional for each component of  $Y^*$  is a truncated normal of the form

$$(2.6) \quad \mathbf{y}_i^* | \mathbf{y}_i = \ell, \text{rest} \sim \mathcal{N}(\mathbf{x}_i \beta, 1) 1\{\mathbf{y}_i^* \in (c_\ell, c_{\ell+1})\}$$

where for subject  $i$ ,  $\mathbf{y}_i^*$  is a vector of latent outcomes,  $\mathbf{y}_i$  is a vector of observed outcomes, and  $\mathbf{x}_i$  is a vector of covariates. The notation  $1\{\cdot\}$  denotes the indicator function and ensures the truncation. Note that the mean is based on the latent space coefficients  $\beta$ , thus coefficients modeled in the wavelet or spline space must first be transformed back. Each cut-point has a uniform full conditional of the form

$$(2.7) \quad c_\ell | \text{rest} \sim \mathcal{U}(a_{c_\ell}, b_{c_\ell})$$

where the max has the form  $a_{c_\ell} = \max\{\max(Y^* | Y = \ell), c_{\ell-1}\}$  and the minimum is  $b_{c_\ell} = \min\{\min(Y^* | Y = \ell + 1), c_{\ell+1}\}$ . We now consider approaches to modeling the latent functional outcome.

**3. Modeling the Latent Functional Outcome.** Given the formulation in (2.5), we can model the  $Y^*$  using functional regression techniques for Gaussian functional outcomes. Typically, we would perform some form of basis expansion to model the functional form of  $\beta$ . Two commonly used sets of basis functions are wavelets and splines. We develop two approaches in the spirit of [Morris and Carroll \(2006\)](#) and [Goldsmith and Kitago \(2016\)](#), utilizing both types of basis functions.

3.1. *Wavelet-based Model Formulation.* Working from the discretized model (2.5) and applying a Discrete Wavelet Transformation (DWT) to the latent outcome gives the decomposition  $Y^* = Y^{*W}W$  where  $Y^{*W}$  is the resulting wavelet-space coefficients and  $W$  is a matrix of wavelet basis functions. Decomposing  $\beta$  gives  $\beta = \beta^W W$  and the DWT applied to  $E$  results in  $E = E^W W$ . Given these, we express model (2.5) as

$$(3.1) \quad Y^{*W}W = X\beta^W W + E^W W.$$

Note that the matrix representations of the wavelet basis are orthogonal, thus  $WW' = I_{T^*}$  where  $T^*$  is the number of wavelet basis functions and  $I_{T^*}$  is a  $T^* \times T^*$  identity matrix. Post-multiplying model (3.1) by  $W'$  gives

$$(3.2) \quad Y^{*W} = X\beta^W + E^W,$$

where  $E^W \sim \mathcal{GP}(0, \Sigma_{E^W})$  for  $\Sigma_E = \Sigma_{E^W} W$ . We now consider prior specifications on the latent model components.

First, we assume independence in the wavelet space which allows model (3.2) to be split up into a series of  $T^*$  separate models for each coefficient in the wavelet space, double-indexed by the wavelet scale,  $j$ , and location,  $k$ . For an  $N \times P$  set of scalar covariates,  $X$ , the independence assumption allows for the sequential fitting of separate models of the form

$$(3.3) \quad \mathbf{y}_{(j,k)}^{*W} = X\boldsymbol{\beta}_{(j,k)}^W + \mathbf{e}_{(j,k)}^W.$$

where  $\mathbf{y}_{(j,k)}^{*W}$  and  $\mathbf{e}_{(j,k)}^W$  are  $N \times 1$  vector components of  $Y^{*W}$  and  $E^W$ , respectively, and  $\boldsymbol{\beta}_{(j,k)}^W$  is a  $P \times 1$  vector of coefficients. We place spike and slab priors on the coefficients  $\boldsymbol{\beta}_{(j,k)}^W = \left\{ \beta_{(p,jk)}^W \right\}$ , where  $p$  indexes the number of columns of  $X$ . The prior on the  $p$ th coefficient from model (3.3) is

$$(3.4) \quad \beta_{(p,jk)}^W \sim \gamma_{(p,jk)} \mathcal{N}(0, \tau_{pj}) + (1 - \gamma_{(p,jk)}) d_0, \quad \gamma_{(p,jk)} \sim \text{Bern}(\pi_{pj}),$$

where  $d_0$  is a point-mass distribution at zero. This adaptive prior performs shrinkage in the wavelet space. The independence assumption and spike and slab priors are consistent with the previous literature on wavelet-based functional regression (Morris and Carroll, 2006; Malloy et al., 2010; Zhu, Brown, and Morris, 2011; Meyer et al., 2015). For the parameters  $\tau_{pj}$  and  $\pi_{pj}$ , we place hyper-priors on  $\tau_{pj} \sim \text{IG}(a_\tau, b_\tau)$  and  $\pi_{pj} \sim \text{Beta}(a_\pi, b_\pi)$ , where the hyper-parameters  $a_\tau, b_\tau, a_\pi$ , and  $b_\pi$  are fixed and based on empirical Bayes estimates. Finally, we place a mean zero normal prior on the  $\mathbf{e}_{(j,k)}^W$  with variance  $\sigma_{(j,k)}^2$ . The covariance induced by this assumption is  $\Sigma_E =$

$W' \Sigma_{EW} W$  which, as shown in [Morris and Carroll \(2006\)](#), encompasses a broad class of covariance structures.

Using these prior specifications, we can describe the full conditionals. For the wavelet-space coefficients, the conditional is a mixture of a normal and a point-mass at zero of the form

$$(3.5) \quad \beta_{(p,jk)}^W | \text{rest} \sim \gamma_{p,jk} N(\mu_{p,jk}, \varepsilon_{p,jk}) + (1 - \gamma_{p,jk}) d_0.$$

The mixture probability,  $\alpha_{p,jk}$ , is given by  $\alpha_{p,jk} = \Pr(\gamma_{p,jk} = 1 | \text{rest}) = O_{p,jk} / (O_{p,jk} + 1)$  for  $O_{p,jk} = \pi_{pj} / (1 - \pi_{pj}) \text{BF}_{p,jk}$  and

$$\text{BF}_{p,jk} = (1 + \tau_{p,jk} / V_{p,jk})^{-1/2} \exp \left\{ \frac{1}{2} \zeta_{p,jk}^2 (1 + V_{p,jk} / \tau_{p,jk}) \right\}.$$

The mean of the normal part of the mixture is  $\mu_{p,jk} = \hat{\beta}_{(p,jk),\text{MLE}}^W (1 + V_{p,jk} / \tau_{p,jk})^{-1}$  and the variance is  $\varepsilon_{p,jk} = V_{p,jk} (1 + V_{p,jk} / \tau_{p,jk})^{-1}$ . The value  $\hat{\beta}_{(p,jk),\text{MLE}}^W$  is taken from an initial estimate using maximum likelihood estimation of the latent variable model and  $V_{p,jk}$  is the variance of  $\hat{\beta}_{(p,jk),\text{MLE}}^W$  which has the form  $(\mathbf{x}_p' \Sigma_{EW} \mathbf{x}_p)^{-1}$  for the  $p$ th column of  $X$ ,  $\mathbf{x}_p$ .

For each  $\mathbf{y}_{(j,k)}^{*W}$ , the conditional of the diagonal elements of  $\Sigma_{EW}$ ,  $\sigma_{(j,k)}^2$ , is

$$(3.6) \quad f(\sigma_{(j,k)}^2 | \text{rest}) \propto f \left\{ \sigma_{(j,k)}^2 \right\} \left\{ \sigma_{(j,k)}^2 \right\}^{-N/2} \times \exp \left\{ -\frac{1}{2\sigma_{(j,k)}^2} (\mathbf{y}_{(j,k)}^{*W} - X\beta_{(j,k)}^W)' (\mathbf{y}_{(j,k)}^{*W} - X\beta_{(j,k)}^W) \right\}.$$

where  $f \left\{ \sigma_{(j,k)}^2 \right\}$  is the prior on the variance components. We select an inverse-gamma prior with parameters  $a_{\sigma^2}$  and  $b_{\sigma^2}$  which we base off of the empirical Bayes estimates. The full conditionals for the regularization parameters are

$$(3.7) \quad \tau_{pj} | \text{rest} \sim IG \left\{ a_\tau + \frac{1}{2} \gamma_{p,jk}, b_\tau + \frac{1}{2} \gamma_{p,jk} \left( \beta_{(p,jk)}^W \right)^2 \right\}$$

$$(3.8) \quad \pi_{pj} | \text{rest} \sim \text{Beta} (a_\pi + \gamma_{p,jk}, b_\pi + \gamma_{p,jk})$$

for  $a_\tau, b_\tau, a_\pi$ , and  $b_\pi$  fixed and estimated via empirical Bayes. All empirical Bayes estimates are as described in [Morris and Carroll \(2006\)](#). Combining these conditionals with the latent conditionals in Section 2.2, the MCMC sampler begins with draws from (2.6) and (2.7). Then we project the  $Y^*$  into the wavelet space and draw  $\beta^W$  from (3.5). Instead of drawing directly



from (3.6) we implement a Metropolis-Hastings step to ensure the variance is not too close to zero. We use a log-normal density as proposal, centered at the current step with variance tuned to achieve an ideal acceptance rate. Finally, we take draws from (3.7) and (3.8).

Use of the DWT requires selecting a type of wavelet, the number of vanishing moments, a boundary padding procedure, and the number of levels of decomposition. Common choices of wavelet type include Daubechies, Symmlets, and Coiflets with varying vanishing moments for the mother wavelets and symmetric half-point, periodic-padding, and zero-padding for the boundary padding. Choice of the mother wavelet and padding will depend largely on the data in question, however Symmlets with eight vanishing moments, also known as least asymmetric wavelets, can be used for most general purposes (Percival and Walden, 2000). In preliminary runs, we found such Symmlets in-conjunction with symmetric half-point padding to be sufficient in most cases and explore two choices of number of levels of decomposition,  $J = 6, 8$ . Both the number of vanishing moments and the level of decomposition will control the smoothness of the estimation with larger values of each resulting in smoother estimates. The fast DWT assumes equally spaced data, which is the case for the rhesus macaques data where  $t$  denotes days during the year. However, Sardy et al. (1999) show that wavelets for equally spaced data can be used if measurements are at least taken on the same, non-equally spaced grid. In this case, the domain of the wavelet basis functions is effectively  $1, \dots, T$  instead of  $t_1, \dots, t_T$ .

*3.2. Spline-based Model Formulation.* We begin again with the discretized model in (2.5) and formulate our spline-based model in the spirit of Goldsmith and Kitago (2016). Let  $\Theta$  denote a  $T \times K$  matrix of basis functions and  $\beta^S$  be a  $K \times P$  matrix of basis coefficients such that  $\beta = (\Theta\beta^S)'$ . To model between curve covariance, we use fPC with  $K_p$  number of scores. Let  $E = C(\Theta\beta^E)' + E^S$  where  $C$  is an  $N \times K_p$  matrix of subject scores,  $\beta^E$  is the  $K \times K_p$  matrix of coefficients, and  $E^S$  is an  $N \times T$  matrix of independent errors. The spline-based model is then

$$(3.9) \quad Y^* = X\beta^{S'}\Theta' + C\beta^{E'}\Theta' + E^S$$

for the  $N \times P$  matrix of scalar covariates,  $X$ . We penalize the fits of both  $\beta^S$  and  $\beta^E$  using a penalty matrix,  $\Delta$ , that is dependent upon choice of spline basis. For B-splines based models, we use the same penalty matrix as in Goldsmith and Kitago (2016):  $\Delta = \eta\Delta_0 + (1 - \eta)\Delta_2$  where  $\Delta_0$  and  $\Delta_2$  are the zeroth and second derivate penalties, respectively. The control parameter  $\eta$  is between 0 and 1 and chosen to strike a balance between

smoothness and shrinkage with values near zero favoring shrinkage. We use  $\eta = 0.01$  for all models using this penalty scheme.

The OPFRM also allows for the use of O’Sullivan penalized splines, or O-splines as we refer to them, which are described in detail in [Wand and Ormerod \(2008\)](#). To construct O-splines, we begin with the standard B-spline expansion using  $K + 4$  knots. The  $(d, d')$  entry of the penalty matrix is  $\Delta_{dd'} = \int_a^b \ddot{\theta}_d(x) \ddot{\theta}_{d'}(x) dx$  where  $\ddot{\theta}$  is the second derivative function of the matrix of basis functions  $\Theta$  for  $x \in \mathbb{R}$  and  $a$  and  $b$  equal to the end points of a non-decreasing sequence of knots. Fitting the model with O-splines in a mixed model framework corresponds to penalizing the fit with the penalty term  $\lambda_d \int_a^b \left\{ \ddot{f}_d(x) \right\}^2 dx$ .

For both sets of penalized splines, we place mean zero normal priors on  $\beta^S$  and  $\beta^E$  with covariances equal to  $\Lambda_S \otimes \Delta$  and  $\Lambda_E \otimes \Delta$ , respectively, where  $\otimes$  denotes the Kronecker product. Both  $\Lambda_S$  and  $\Lambda_E$  are diagonal matrices with the diagonal elements equal to  $\lambda_{k,S}^{-1}$  and  $\lambda_{k_p,E}^{-1}$  for the  $k$ th basis function and  $k_p$ th fPC basis function. We also place a mean zero normal prior on each row of  $C$  with variance  $I_{K_p}$ , the  $K_p \times K_p$  identity matrix. Finally, we let the rows of  $E^S$  vary independently with mean zero and variance  $\sigma_E^2 I_T$  where  $I_T$  is the  $T \times T$  identity matrix. Such specifications are consistent with prior work on spline-based function-on-scalar regression such as [Goldsmith, Zipunnikov, and Schrack \(2015\)](#), [Goldsmith and Kitago \(2016\)](#), and references therein.

The resulting full conditionals using either B-splines or O-splines are the same, varying only in the size of  $\Theta$  and the form of the penalty matrix,  $\Delta$ . The conditional for  $\beta^S$  is normal with the form

$$(3.10) \quad \beta^S | \text{rest} \sim N(\mu_{\beta^S}, \Sigma_{\beta^S})$$

where  $\Sigma_{\beta^S} = \left[ \frac{1}{\sigma_E^2} \{ (X'X) \otimes (\Theta'\Theta) \} + (\Lambda_S \otimes \Delta) \right]^{-1}$  and  $\mu_{\beta^S} = \frac{1}{\sigma_E^2} \Sigma_{\beta^S} (X \otimes \Theta)' (\vec{Y}^* - \vec{P})$  for the vectorized current  $Y^*$  and fPC components,  $\vec{Y}^*$  and  $\vec{P}$  respectively. That is,  $\vec{P}$  is equal to the vectorized current, evaluated step of  $C\beta^{E'}\Theta'$ . For the fPC coefficients, the conditional is also normal:

$$(3.11) \quad \beta^E | \text{rest} \sim N(\mu_{\beta^E}, \Sigma_{\beta^E})$$

where  $\Sigma_{\beta^E} = \left[ \frac{1}{\sigma_E^2} \{ (C'C) \otimes (\Theta'\Theta) \} + (\Lambda_E \otimes \Delta) \right]^{-1}$  and  $\mu_{\beta^E} = \frac{1}{\sigma_E^2} \Sigma_{\beta^E} (C \otimes \Theta)' (\vec{Y}^* - \vec{B})$  for  $\vec{Y}^*$  as previously defined and  $\vec{B}$  equal to the vectorized current, evaluated step of  $X\beta^{S'}\Theta'$ . For each subject, the conditionals of the rows of  $C$ ,  $\mathbf{c}_i$ , are normal

$$(3.12) \quad \mathbf{c}_i | \text{rest} \sim N(\mu_{\mathbf{c}_i}, \Sigma_{\mathbf{c}_i}),$$

for  $\Sigma_{\mathbf{c}_i} = \left\{ \frac{1}{\sigma_E^2} (\Theta \beta^E)' (\Theta \beta^E) + I_{K_p} \right\}^{-1}$  and  $\mu_{\mathbf{c}_i} = \frac{1}{\sigma_E^2} \Sigma_{\mathbf{c}_i} (\Theta \beta^E)' (\mathbf{y}_i^* - \mathbf{x}_i \beta^S)$ .

The conditionals for the variance  $\sigma_E^2$  and diagonals of  $\Lambda_S$  and  $\Lambda_E$  are

$$(3.13) \quad \sigma_E^2 | \text{rest} \sim IG \left\{ A_\sigma + \frac{NT}{2}, B_\sigma + \sum_{i=1}^N \left( \mathbf{y}_i^* - \mathbf{x}_i \beta^{S'} \Theta' - \mathbf{c}_i \beta^{E'} \Theta' \right)^2 \right\},$$

$$(3.14) \quad \lambda_{k,S} | \text{rest} \sim IG \left( A_S + \frac{K}{2}, B_{k,S} + \frac{1}{2} \beta_k^{S'} \Delta \beta_k^S \right) \text{ and}$$

$$(3.15)$$

$$\lambda_{k_p,E} | \text{rest} \sim IG \left( A_E + \frac{K_p}{2}, B_E + \frac{1}{2} \beta_{k_p}^{E'} \Delta \beta_{k_p}^E \right)$$

where  $\beta_k^S$  and  $\beta_{k_p}^E$  denote the  $k$ th and  $k_p$ th rows of the matrices  $\beta^S$  and  $\beta^E$ . We take  $A_\sigma$  and  $B_\sigma$  to both be 1,  $A_E = K_p/2$ ,  $B_E = K_p/2$ , and  $A_S = K/2$ . The parameter  $B_S$  is the larger of 1 and  $(1/2) \hat{\beta}_k^{S'} \Delta \hat{\beta}_k^S$ , where  $\hat{\beta}_k^S$  is the least squares estimate, as suggested by [Goldsmith and Kitago \(2016\)](#). For the spline-based models, the sampler begins with (2.6) and (2.7) and then steps through (3.10) to (3.15). For both spline bases, we must select the number of basis functions for both the fixed effects and the fPC components. We use two different values of knots for B-splines,  $K = 5, 10$ , two different values for the O-splines,  $K = 2, 4$ , and let  $K_p = 2$  for all settings.

**3.3. Interval Estimation.** We implement two types of intervals for describing uncertainty regarding the estimate of  $\beta$ . First is a point-wise credible interval approach and second is a joint-credible interval as described by [Ruppert, Wand, and Carroll \(2003\)](#). To construct point-wise intervals, we find the usual  $100(1 - \alpha/2)\%$  credible interval at each  $t$  for each  $\beta(t)$ . The resulting intervals constitute the whole 95% credible interval for the curve. For the joint-credible intervals, let  $\hat{\beta}(t)$  and  $\widehat{\text{St.Dev}} \{ \hat{\beta}(t) \}$  denote the mean and standard deviations of the posterior samples of  $\beta(t)$ . We then construct the interval  $I_\alpha(t) = \hat{\beta}(t) \pm q_{(1-\alpha)} \left[ \widehat{\text{St.Dev}} \{ \hat{\beta}(t) \} \right]$  where  $q_{(1-\alpha)}$  is the  $(1 - \alpha)$  quantile taken over the  $M$  MCMC samples of the quantity  $Z^{(m)} = \max_{t \in \mathcal{T}} \left| \frac{\beta^{(m)}(t) - \hat{\beta}(t)}{\widehat{\text{St.Dev}} \{ \hat{\beta}(t) \}} \right|$ . Both approaches have previously been used in the Bayesian functional regression with, for example, [Goldsmith, Zipunikov, and Schrack \(2015\)](#) and [Goldsmith and Kitago \(2016\)](#) implementing the point-wise approach and [Meyer et al. \(2015\)](#) and [Lee et al. \(2018\)](#) implementing the joint-interval approach. Two testing procedures, Bayesian False Discovery Rate and Simultaneous Band Scores, implemented in previous works, [Malloy et al. \(2010\)](#), [Meyer et al. \(2015\)](#), and references therein

are also available for use in the OPFRM but not discussed here, see the Supplementary Material for additional details.

**4. Simulation Study.** To investigate the operating characteristics of the OPFRM, we construct simulated scenarios designed to mimic possible computer-use patterns in rhesus macaques over the course of the year. To this end, we develop four “true” curve settings to simulate ordinal functional outcomes from a single covariate,  $x_i$ , which we draw from a standard normal. We refer to the curves as the sigmoidal, seasonal, decay, and peak settings. Each of these settings suggest different patterns of usage over the course of the year. For example, in the sigmoidal setting, changes in usage associated with a positive change in  $x_i$  slowly increase over the course of the year while in the seasonal setting, usage varies with the time of year. Under these four settings, we generate functional curves using three different underlying covariance structures to mimic with-in curve association. The three structures we consider are independent (least realistic), exponential (most realistic), and compound symmetric, also called exchangeable. Using these curves and structures, we generate  $N = 40$  ordinal functional outcome curves from a multinomial distribution with  $L = 4$ . The functions describing each curve setting and covariance structure are in the Supplementary Material.

For each curve and covariance structure combination, we generate 200 datasets and run six models using B-spline with  $K = 5$  and 10, O-spline with  $K = 2$  and 4, and Symmlets on 8 vanishing moments and levels  $J = 6$  and 8. We take 1000 total posterior samples for each model, discarding the first 500. Runtimes for the full 1000 samples vary by basis type but B-spline models typically take between 12.51 seconds and 13.50 seconds and O-spline models take between 12.78 and 13.13 seconds. Wavelet models take considerably longer running between 93.79 and 106.93 seconds. We run models on a laptop with a 2.9 GHz Intel Core i5 processor with 16 GB of memory. All computation is done using MATLAB version R2017a.

Due to space constraints, we present tabular results for only the sigmoidal and seasonal settings and graphical results for only those two settings under the exponential covariance structure. Average mean integrated squared error (MISE) for each scenario is in Table 1 while mean point-wise coverage probabilities are in Table 2. Figures 1 and 2 contain posterior estimates for each simulated dataset plotted along with the average across all datasets as well as the true curve. In Table 1, the smallest average MISE is bolded and second smallest is italicized. Looking by scenario, we see that the O-spline model with  $K = 2$  typically performs the best with the  $K = 4$  model performing second best. The wavelet-based model with  $J = 6$  levels also per-

TABLE 1

*MISE for each model under the sigmoidal and seasonal scenarios averaged over all 200 datasets. Bold-faced entries denote the lowest value at each Setting and Covariance Structure, Cov. Str., combination. Italicized entries denote the second smallest value. The abbreviations Ind., Exp., C. S., and P. W. refer to Independence, Exponential, Compound Symmetric, and Point Wise, respectively.*

<i>Setting</i>	<i>Cov. Str.</i>	<i>B-Spline</i>		<i>O-Spline</i>		<i>Symmlets</i>	
		<i>K = 5</i>	<i>K = 10</i>	<i>K = 2</i>	<i>K = 4</i>	<i>J = 6</i>	<i>J = 8</i>
Sigmoidal	Ind.	0.0022	0.0014	<i>0.0010</i>	0.0012	<b>0.0009</b>	0.0033
	Exp.	0.0024	0.0017	<b>0.0012</b>	<i>0.0014</i>	<b>0.0012</b>	0.0035
	C. S.	0.0023	0.0016	<b>0.0010</b>	0.0013	<i>0.0011</i>	0.0034
Seasonal	Ind.	0.0053	0.0015	<b>0.0010</b>	<i>0.0012</i>	0.0023	0.0033
	Exp.	0.0056	0.0019	<b>0.0014</b>	<i>0.0016</i>	0.0028	0.0034
	C. S.	0.0054	0.0017	<b>0.0011</b>	<i>0.0014</i>	0.0025	0.0034

forms well under the sigmoidal setting and the B-spline model with  $K = 10$  is typically third best in terms of MISE. Figures 1 and 2 reinforce this with the O-spline models best capturing the true curve and the  $K = 10$  B-spline and Symmlet  $J = 6$  models performing reasonably well. Similar graphics presenting the estimated curves under the independent and compound symmetric structures are in the Supplementary Material. Looking within model, the underlying covariance structure does not appear to have too strong an effect on estimation, though the MISE is largest when the true structure is exponential and smallest when it is independent. Within basis-type, the B-spline model with more  $K = 10$  knots performs better than with  $K = 5$  knots. For the O-spline models, fewer knots produces a better fit though the MISEs are close to each other. When using Symmlet wavelets, the model with fewer levels performs best.

We primarily assess both the 95% joint and 95% point-wise credible intervals approaches using mean point-wise coverage probabilities. We calculate coverage by checking if the truth is contained in the interval at each  $t$ , averaging over all  $t$  to obtain a mean coverage for each simulated dataset. Finally, we take the average of these values over all 200 datasets. Table 2 presents these results with the largest coverage probabilities in bold and second largest italicized. Here we see that, regardless of scenario, mean point-wise coverage is best for the joint interval using Symmlets with  $J = 6$  levels of decomposition with the second best coverage belonging to the joint intervals from the B-spline model with  $K = 10$  knots. However, with the exception of the B-spline model with only  $K = 5$  knots, all joint intervals achieve the nominal coverage. None of the point-wise intervals achieve the nominal level, though some are close particularly for the  $K = 10$  B-spline and both O-spline models. The underlying covariance structure of the func-

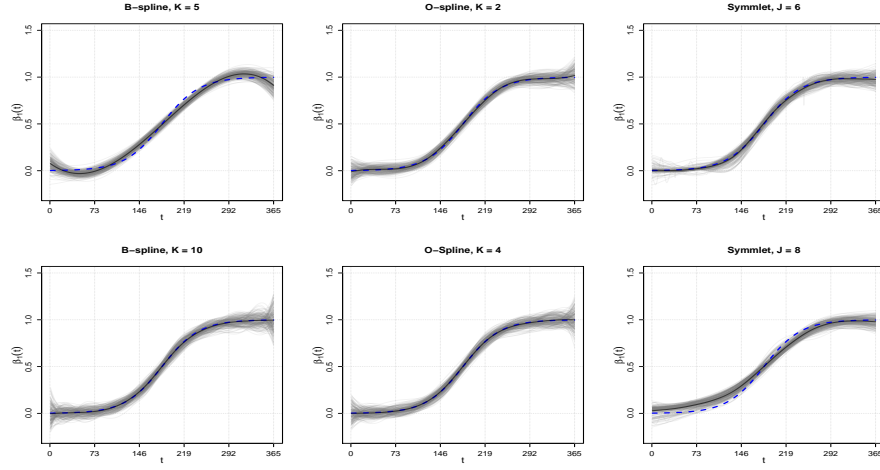


FIG 1. Posterior estimates for the sigmoidal setting under the exponential covariance structure from each simulated dataset are in light gray. Solid black curves depict the average estimate over all 200 datasets while the dashed blue curves are the truth. The first column shows estimates from B-spline models, second columns O-spline, and third column Symmlet. The top row shows the lower number of splines or level of decomposition, bottom row contains higher. This figure appears in color in the electronic version of this article.

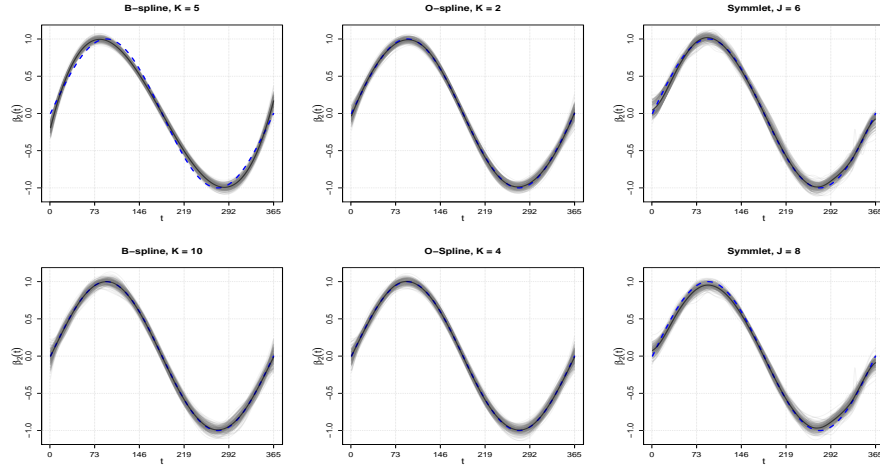


FIG 2. Posterior estimates for the seasonal setting under the exponential covariance structure from each simulated dataset are in light gray. Solid black curves depict the average estimate over all 200 datasets while the dashed blue curves are the truth. The first column shows estimates from B-spline models, second columns O-spline, and third column Symmlet. The top row shows the lower number of splines or level of decomposition, bottom row contains higher. This figure appears in color in the electronic version of this article.

TABLE 2

Mean point-wise coverage probabilities of the 95% joint and 95% point-wise credible intervals for each model under the sigmoidal and seasonal scenarios averaged over all 200 datasets. Bold-faced entries denote the largest value at each Setting and Covariance Structure, Cov. Str., combination for both interval types. Italicized entries denote the second largest value. The abbreviations Ind., Exp., C. S., and P. W. refer to Independence, Exponential, Compound Symmetric, and Point Wise, respectively.

Setting	Cov. Str.	Int.	B-Spline		O-Spline		Symmlets	
			$K = 5$	$K = 10$	$K = 2$	$K = 4$	$J = 6$	$J = 8$
Sigmoidal	Ind.	Joint	0.8560	<i>0.9986</i>	0.9942	0.9972	<b>1.0000</b>	0.9727
		P. W.	0.6681	0.9490	0.9330	0.9452	0.9432	0.7798
	Exp.	Joint	0.8352	<i>0.9957</i>	0.9849	0.9938	<b>0.9997</b>	0.9727
		P. W.	0.6488	0.9304	0.8955	0.9169	0.9224	0.7745
	C. S.	Joint	0.8479	<i>0.9963</i>	0.9905	0.9961	<b>0.9992</b>	0.9763
		P. W.	0.6595	0.9340	0.9161	0.9322	0.9350	0.7868
Seasonal	Ind.	Joint	0.5988	<i>0.9968</i>	0.9922	0.9965	<b>0.9974</b>	0.9952
		P. W.	0.4048	0.9417	0.9343	0.9404	0.8998	0.9127
	Exp.	Joint	0.5985	<i>0.9918</i>	0.9793	0.9880	<b>0.9962</b>	0.9944
		P. W.	0.4129	0.9093	0.8756	0.9032	0.8807	0.9084
	C. S.	Joint	0.5997	<i>0.9938</i>	0.9889	0.9928	<b>0.9979</b>	0.9955
		P. W.	0.4093	0.9291	0.9126	0.9247	0.8942	0.9124

tional outcome does appear to affect coverage with coverage decreasing for both interval types as the structure gets more complicated. We also present joint coverage probabilities, where coverage is calculated as the percent of simulated results whose intervals contain the whole true curve, and the average width of the credible intervals in the Supplementary Material. The joint coverage is highest for the joint intervals using O-splines with  $K = 4$  and Symmlets with  $J = 6$  while average interval widths are smallest for the point-wise intervals. However, when using the O-spline based models, the joint intervals are similar in width.

**5. Application.** We now present the results of our analysis of the computer-use data. We restrict our investigation to the first full year available for analysis, encompassing all four seasons for the monkeys: the breeding season, winter, birthing season, and summer. In total, we have 72 monkeys available for analysis. Of interest is the effect the the demographic factors sex, rank, and age over the course of the year. Prior to modeling, we center both rank and age. The latent model we fit is  $Y_i^*(t) = \text{sex}_i\beta_1(t) + \text{rank}_i\beta_2(t) + \text{age}_i\beta_3(t) + E_i(t)$  where  $\text{sex}_i$  is an indicator equal to 1 if the monkey is male and 0 if female. The observed ordinal outcome has  $L = 4$  levels corresponding to no usage, low usage, moderate usage, and high usage on day  $t$ . For each monkey, we have 365 total functional observations.

TABLE 3

*Predictive accuracy by holdout set from six-fold cross validation and overall. Table values represent the median percent of holdout set outcomes that are correctly predicted with the median taken over all posterior estimates. Overall values are the median predictive accuracy taken over all holdout sets.*

<i>Holdout Set</i>	<i>B-Spline</i>		<i>O-Spline</i>		<i>Symmlets</i>	
	$K = 5$	$K = 10$	$K = 2$	$K = 4$	$J = 6$	$J = 8$
1	0.6064	0.6041	0.6066	0.6009	0.6187	0.6192
2	0.5502	0.5443	0.5489	0.5463	0.5623	0.5621
3	0.5530	0.5493	0.5573	0.5514	0.5662	0.5662
4	0.4500	0.4550	0.4498	0.4534	0.4514	0.4539
5	0.5582	0.5507	0.5616	0.5589	0.5861	0.5858
6	0.6347	0.6347	0.6347	0.6347	0.6326	0.6347
Overall	0.5580	0.5511	0.5600	0.5566	0.5667	0.5668

The variable  $\text{age}_i$  is the age at which the monkeys received their RFID chip and thus eligible to use the computer system.

We use six-fold cross validation to determine the predictive accuracy of all models where we calculate predictive accuracy as the percent of observed outcomes in the holdout sets correctly predicted by each model. To obtain suitable convergence, each spline-based model is fit on 3000 total samples and the wavelet-based models are fit on 4500 total samples. A discussion of both the validation procedure and model convergence is found in the Supplementary Material. The prediction accuracy for each holdout set and over all sets is in Table 3. The O-spline with  $K = 2$  and both wavelet-based models have the best overall predictive accuracy, however all models demonstrate approximately the same accuracy with only a 1.56% between the smallest and largest overall prediction.

Given the performance of the O-spline model with  $K = 2$  in the simulation study as well as its predictive accuracy, we focus our analysis on this model and present the results from the other models in the Supplementary Material. We refit the model on the whole dataset using 3000 total samples, discarding the first 1500. Computation time for the full models is between 1 to 1.5 minutes for the spline-based models and 14 to 16 minutes for the wavelet-based model. Figure 3 presents the posterior mean (solid blue curve) along with 95% point-wise (shaded blue band) and joint credible (shaded gray band) intervals. We also note which coefficients are deemed significant by each procedure in the top (point-wise) and bottom (joint) rugs.

From Figure 3, we see that both the sex and age of a monkey significantly contribute to its daily usage over the course of the year. Male monkeys consistently use the computers less than female monkeys and older monkeys use the computers less than younger monkeys. These patterns vary over the



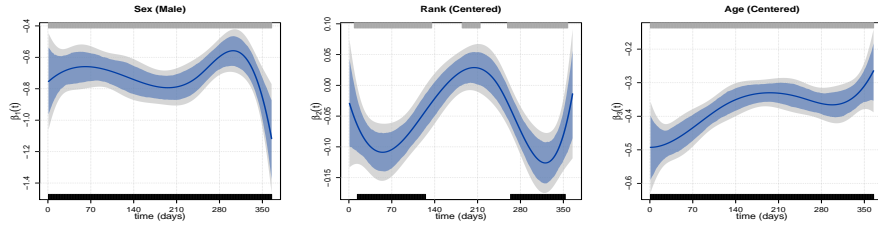


FIG 3. *Posterior estimates and intervals of demographic factors from the O-spline,  $K = 2$  model. The solid blue curves indicate the posterior mean of  $\beta(t)$  while the shaded blue bands denote the 95% point-wise credible interval. The 95% joint credible interval is the slightly larger shaded gray band. The rugs denote coefficients deemed significant by the point-wise (top) and join (bottom) intervals. This figure appears in color in the electronic version of this article.*

course of the year, but for each variable the effect is significantly less than zero for the duration of the year. Rank does play a role in usage, although it is minor by comparison and only significant during certain periods of the year. In particular, higher ranking monkeys appear to use the computers less during the breeding season and the the summer season. The effects during these periods are significant, however the changes are much smaller with coefficients mostly ranging between  $-0.01$  and  $-0.15$ . By comparison, the effects of a monkey's sex and age are much stronger.

**6. Discussion.** While recent functional literature delves into non Gaussian outcomes, more work is needed to expand the reach of available methodology. For ordinal functional outcomes, the literature is quite sparse consisting of only one limited investigation and no publicly available code. In this work, we address this gap by introducing the OPFRM which can accommodate ordinal outcomes of any level. The OPFRM is flexible as it allows for the choice of basis function, either B-splines or discrete wavelets of any type, which are commonly used in the literature. It also allows for the use of O-splines which, to the best of our knowledge, have not been previously implemented in generalized function-on-scalar regression. Building on the frameworks of [Morris and Carroll \(2006\)](#) and [Goldsmith and Kitago \(2016\)](#), both spline- and wavelet-based formulations of the model account for within curve correlations within the basis-transformed latent space either via the use of fPC or the whitening property of the DWT. The OPFRM also allows for a potentially large number of functional observations and any combination of continuous and discrete scalar covariates.

In simulation, we investigate the operating characteristics of the OPFRM

using a reasonable sample size of  $N = 40$  under four different curve conditions for three different underlying correlation structures. While the O-splines perform best in terms of MISE, we show that the model performs well in estimation under any basis choice as MISE is comparable using Symmlets with  $J = 6$  or B-splines with  $K = 10$ . Varying the underlying correlation structure from independent to time-invariant to time-varying does not have a significant impact on estimation which illustrates the ability of both the DWT and fPC to capture within curve correlation in the latent space. We show that coverage for both point-wise and joint credible intervals can be affected when using B-splines with too few basis functions. The point-wise intervals perform best when the underlying covariance structure is independent while the joint intervals consistently provide the highest coverage. Applying the OPFRM to the monkey computer use data, we demonstrate the predictive accuracy of each basis function showing that the models perform similarly. We show that two of the demographic factors of interest, a monkey's sex and age, are significantly associated with usage for the duration of the year. The third factor, rank, has periods of significance early and late in the year. However the effect size is quite small, suggesting the effect of rank, while significant, is minimal.

To summarize, the OPFRM is a flexible modeling framework for ordinal functional outcomes. The model performs well in simulation and application under any choice of basis function and is computationally efficient, particularly for the spline-based models. Our application has relatively smooth signals thus a spline-based approach makes sense with the O-splines allowing us to use fewer basis functions, and therefore fewer coefficients, than the B-spline models. The wavelet-based models are preferred when the signal is spiky and irregular and splines may over smooth. Thus the flexibility in choice of basis function in the OPFRM is useful in allowing us to determine the the best basis function for the application all in one modeling framework. Further work is needed to explore extensions to the generalized function-on-function setting as well as the introduction of other basis functions. The model also currently uses the probit link and assumes proportionality when moving from one outcome category to the next. Finally, we assume the sampled curves are complete and not missing any values. Future work will seek to address these limitations.

## SUPPLEMENTARY MATERIAL

### Supplement A: Additional Details and Results

(<http://www.e-publications.org/ims/support/download/imsart-ims.zip>). Supporting material to Sections 3–5 is available alongside this article.

## REFERENCES

- Albert, J. H. and Chib, S. (1993). Bayesian analysis of binary and polychotomous response data. *Journal of the American Statistical Association* **88**, 669–679. [MR1224394](#)
- Chen, Y., Goldsmith, J., and Ogden, R. T. (2016). Variable selection in function-on-scalar regression. *Stat.* **5** 88–101. [MR3478799](#)
- Faraway, J. J. (1997). Regression analysis for a functional response. *Technometrics* **39**, 254–261. [MR1462586](#)
- Gazes, R. P., Brown, E. K., Basile, B. M., and Hampton, R. R. (2013). Automated cognitive testing of monkeys in social groups yields results comparable to individual laboratory based testing. *Animal Cognition* **16**, 445–458.
- Gertheiss, J., Maier, V., Hessel, E. F., and Staicu, A.-M. (2015). Marginal functional regression models for analyzing the feeding behavior of pigs. *Journal of Agricultural, Biological, and Environmental Statistics* **20**, 353–370. [MR3396556](#)
- Goldsmith, J., and Kitago, T. (2016). Assessing systematic effects of stroke on motorcontrol by using hierarchical function-on-scalar regression. *Journal of the Royal Statistical Society Series C* **65**, 215–236. [MR3456686](#)
- Goldsmith, J., and Schwartz, J. E. (2017). Variable selection in the functional linear concurrent model. *Statistics in Medicine* **36**, 2237–2250. [MR3660128](#)
- Goldsmith, J., Zipunnikov, V., and Schrack, J. (2015). Generalized multilevel function-on-scalar regression and principal component analysis. *Biometrics* **71**, 344–353. [MR3366239](#)
- Guo, W. (2002). Functional mixed effects models. *Biometrics* **58**, 121–128. [MR1891050](#)
- Hall, P., Müller, H.-G., and Yao, F. (2008). Modelling sparse generalized longitudinal observations with latent Gaussian processes. *Journal of the Royal Statistical Society Series B* **70**, 703–723. [MR2523900](#)
- Krafty R. T., Gimotty, P. A., Holtz, D., Coukos, G., and Guo, W. (2008). Varying-Coefficient Model with Unknown Within-Subject Covariance for the Analysis of Tumor Growth Curves. *Biometrics* **64**, 1023–1031. [MR2522249](#)
- Lee, W., Miranda, M. F., Rausch, P., Baladandayuthapani, V., Fazio, M., Downs, J. C., and Morris, J. S. (2018). Bayesian semiparametric functional mixed models for serially correlated functional data, with application to glaucoma data. *Journal of the American Statistical Association*, to appear <https://doi.org/10.1080/01621459.2018.1476242>
- Li, G., Huang, J. Z., and Shen, H. (2018). Exponential Family Functional Data Analysis via a Low-Rank Model. *Biometrics* <https://doi-org.proxy.library.georgetown.edu/10.1111/biom.12885>.
- Li, H. C., Staudenmayer, J., and Carroll, R. J. (2014). Hierarchical Functional Data with Mixed Continuous and Binary Measurements. *Biometrics* **70**, 802–811. [MR3295741](#)
- Malloy, E. J., Morris, J. S., Adar, S. D., Suh, H., Gold, D. R., and Coull, B. A. (2010). Wavelet-based functional linear mixed models: an application to measurement error-corrected distributed lag models. *Biostatistics* **11**, 432–452.
- Meyer, M. J., Coull, B. A., Versace, F., Cinciripini, P., and Morris, J. S. (2015). Bayesian function-on-function regression for multilevel functional data. *Biometrics* **71**, 563–574. [MR3402592](#)
- Morris, J. S. (2015). Functional regression. *Annual Reviews of Statistics and its Application* **2**, 321–359.
- Morris, J. S. and Carroll, R. J. (2006). Wavelet-based functional mixed models. *Journal of the Royal Statistical Society Series B* **68**, 179–199. [MR2188981](#)
- Percival, D. B. and Walden, A. T. (2000). *Wavelet Methods for Time Series Analysis* (Cambridge Series in Statistical and Probabilistic Mathematics), Cambridge: Cam-

- bridge University Press.
- Ramsay, J. O. and Silverman, B. W. (1997). *Functional Data Analysis* (1st ed.), New York: Springer-Verlag.
- Reiss, P.T., Huang, L., and Mennes, M. (2010). Fast function-on-scalar regression with penalized basis expansions. *International Journal of Biostatistics* **6**, article 28. [MR2683940](#)
- Ruppert, D., Wand, M. P., and Carroll, R. J. (2003). *Semiparametric Regression*. Cambridge University Press.
- Sardy, S., Percival, D. B., Bruce, A. G., Gao, H.-Y., and Stuetzle, W. (1999). Wavelet shrinkage for unequally spaced data. *Statistics and Computing* **9**, 65–77.
- Scheipl, F., Gertheiss, J., and Greven, S. (2016). Generalized functional additive mixed models. *Electronic Journal of Statistics* **10**, 1455–1492. [MR3507370](#)
- Scheipl, F., Staicu, A. M., and Greven, S. (2015). Functional additive mixed models. *Journal of Computational and Graphical Statistics* **24**, 477–501. [MR3357391](#)
- Shi, J. Q., Wang, B., Murray-Smith, R., and Titterton, D. M. (2007). Gaussian process functional regression modeling for batch data. *Biometrics* **63**, 714–723. [MR2395708](#)
- van der Linde, A. (2009). A Bayesian latent variable approach to functional principal components analysis with binary and count data. *ASTA-Advances in Statistical Analysis* **93**, 307–333. [MR2545698](#)
- van der Linde, A. (2011). Reduced rank regression models with latent variables in Bayesian functional data analysis. *Bayesian Analysis* **6**, 77–126. [MR2781809](#)
- Wand, M. P., and Ormerod, J. T. (2008). On semiparametric regression with O’Sullivan penalized splines. *Australian & New Zealand Journal of Statistics* **50**, 179–198. [MR2431193](#)
- Wang, B., and Shi, J. Q. (2014). Generalized Gaussian Process Regression Model for Non-Gaussian Functional Data. *Journal of the American Statistical Association* **109**, 1123–1133. [MR3265685](#)
- Zhu H., Brown, P. J., and Morris, J. S. (2011). Robust, adaptive functional regression in functional mixed model framework. *Journal of the American Statistical Association* **106**, 1167–1179. [MR2894772](#)
- Zhu H., Brown, P. J., and Morris, J. S. (2012). Robust classification of functional and quantitative image data using functional mixed models. *Biometrics* **68**, 1260–1268. [MR3040032](#)

M. J. MEYER  
DEPARTMENT OF MATHEMATICS AND STATISTICS  
GEORGETOWN UNIVERSITY  
WASHINGTON, DISTRICT OF COLUMBIA 20057  
USA  
E-MAIL: [mjm556@georgetown.edu](mailto:mjm556@georgetown.edu)

R. PAXTON GAZES  
DEPARTMENT OF PSYCHOLOGY  
AND PROGRAM IN ANIMAL BEHAVIOR  
BUCKNELL UNIVERSITY  
LEWISBURG, PENNSYLVANIA 17837  
USA

J. S. MORRIS  
DEPARTMENT OF BIostatISTICS  
THE UNIVERSITY OF TEXAS MD ANDERSON CANCER CENTERS  
HOUSTON, TEXAS 77230  
USA

R. R. HAMPTON  
DEPARTMENT OF PSYCHOLOGY  
EMORY UNIVERSITY AND  
YERKES NATIONAL PRIMATE RESEARCH CENTER  
ATLANTA, GEORGIA 30322  
USA

B. A. COULL  
DEPARTMENT OF BIostatISTICS  
HARVARD T.H. CHAN SCHOOL OF PUBLIC HEALTH  
BOSTON, MASSACHUSETTS 02115  
USA